Title:

Density-dependent attributes of schooling in small pelagic fishes

Authors:

Sho Furuichi[1]*, Yasuhiro Kamimura[1], Masahiro Suzuki[1], Ryuji Yukami[1]

Affiliations:

[1]Fisheries Resources Institute, Japan Fisheries Research and Education Agency, Yokohama, Japan

***Correspondence:**

Name: Sho Furuichi

Full postal address: Fisheries Resources Institute, Japan Fisheries Research and Education Agency, 2-12-4, Fukuura, Kanazawa, Yokohama 236-8648, Japan

Email: sfuru@affrc.go.jp

Funding information:

Funding for this study was provided by the Japan Fisheries Research and Education Agency and the Fisheries Agency of Japan.

ABSTRACT

Many small pelagic fishes obligately form schools; some of these schools attain a remarkable size. Although the school is a fundamental and important ecological unit and is the site of biological interactions such as competition and predation, information on schooling processes in the field remains scarce. Here, we examined the quantitative relationships between population density and school size, the number of schools, and other school characteristics (i.e., packing density, volume, and cross-sectional area) in three species of small pelagic fishes: chub mackerel *Scomber japonicus*, Japanese sardine *Sardinops melanostictus*, and Japanese anchovy *Engraulis japonicus*. We found that school size increased almost linearly with population density, whereas the number of schools and other characteristics increased non-linearly with population density, whereby the rate of increase slowed radically as population density increased. These results indicate that, at low population densities, an increase in density causes an increase in both school size and the number of schools, whereas at higher population densities, an increase in density triggers the formation of larger schools rather than more schools. Furthermore, we found that the shapes of the relationships of all school characteristics with population density differed among species. Our results indicate that the schooling behaviour of small pelagic fishes is density-dependent, and responses to changes in density are species-specific. Our results provide insight into of how biological interactions such as intra- and inter-specific competition and predator-prey interactions mediate the density-dependent processes that underlie the population dynamics and community structure of small pelagic fishes in marine ecosystems.

KEY WORDS:

pelagic fish, schooling, group living, density dependence, western North Pacific

1. INTRODUCTION

Group living is a widespread phenomenon across the animal kingdom (Krause & Ruxton, 2002; Ward & Webster, 2016), and is particularly important in fishes. Most fish species form groups at some stage of their life history, and fishes display more diverse grouping behaviour and a greater range of group sizes and shapes than other taxa (Pavlov & Kasumyan, 2000; Vicsek & Zafeiris, 2012).

Among fishes, the grouping behaviour of small pelagic fishes is especially distinctive and ecologically important. Many small pelagic fishes obligately aggregate to form schools, shoals, or swarms (hereafter, simply 'schools', although the terms are not strictly synonymous), and they often form massive schools consisting of thousands or even millions of individuals (Makris *et al.*, 2006; Misund, 1993). Small pelagic fishes are also important components of marine ecosystems that link lower trophic-level plankton to upper trophic-level predators (Bakun, 2006; Cury *et al.*, 2000; Rice, 1995), and the formation of massive schools by small pelagic fishes is likely to determine population dynamics, community structure, and energy flow in marine ecosystems through processes such as intra- and inter-specific competition and predator–prey interaction (Maury, 2017; Maury & Poggiale, 2013). Therefore, clarifying how and under what conditions small pelagic fishes form massive schools is necessary to better understand marine ecosystem dynamics.

Population density is one of the most fundamental factors affecting school size. An increase in population density leads to a higher encounter rate between conspecific individuals or schools and hence an increased opportunity for school fusion. Therefore, mean school size is expected to increase with population density (Hensor *et al.*, 2005; Niwa, 2004). However, the formation of schools involves not only benefits (e.g., avoiding predation) but also costs (e.g., competition for food), meaning that there is likely to be an optimum school size that allows individuals to maximize their net benefit (Krause & Ruxton, 2002; Ward &

Webster, 2016), and it has been suggested that individuals adjust their schooling behaviour toward this optimum (Sibly, 1983). Therefore, school sizes might converge to a stable size or remain constant regardless of population density, rather than simply increasing in direct proportion to population density (Sibly, 1983).

The relationships between population density and school size are not simple and need to be verified by field or experimental observations. However, field or experimental studies on the relationships between these factors in small pelagic fishes remain scarce. One of the few relevant studies reported that in Atlantic herring (*Clupea harengus*), the spatial size (i.e., cross-sectional area) of schools is relatively stable, and only the number of schools increases as population density increases (Jech & Stroman, 2012). On the other hand, for several small pelagic fishes in Europe, it has been reported that as population density increases, the proportion of spatially large schools increases (Petitgas *et al.*, 2001) as does the number of schools (Brierley & Cox, 2015). Therefore, in small pelagic fishes, the relationship between population density and school size remains unclear, and quantitative relationships between population density and school size have not been well established.

The purpose of this study is to identify quantitative relationships between population density and school size, the number of schools, and other schooling characteristics in three small pelagic fishes: chub mackerel *Scomber japonicus* Houttuyn 1782, Japanese sardine *Sardinops melanostictus* (Temminck & Schlegel 1846), and Japanese anchovy *Engraulis japonicus* Temminck & Schlegel 1846. These three species inhabit the western North Pacific around Japan and are important fisheries resources that account for the majority of total fisheries catch by weight in Japan (Yatsu, 2019). The stock abundance of the three species has fluctuated widely in the last decades (Yatsu, 2019), which allows us to observe a wide range of population densities in the field.

First, to examine whether school characteristics (school size, number of schools, school

packing density, school volume, and school cross-sectional area) increase or remain constant as population density increases and whether the shapes of the relationships are linear or non-linear (e.g., saturating), we fitted power-law models to the relationships between school characteristics and local population density at the feeding grounds of the three small pelagic fishes. Second, to examine whether the relationships between population density and school characteristics are different among species, we compared models with species-specific and species-common relationships.

2. MATERIALS AND METHODS

2.1 Survey

The Japan Fisheries Research and Education Agency has conducted trawl-acoustic surveys to examine the densities and distributions of small pelagic fishes every year since 2005 between September and October in the western North Pacific off northern Japan and the Kuril Islands (Figure 1). The study area corresponds to the feeding grounds of the study species during the months surveyed. In this study, we used data from 2007, when the survey design was established, to 2021, the most recent year available. The specifications of the trawl net are as follows: opening dimensions, 30 m × 30 m; cod-end mesh aperture, 17.5 mm; tow duration, 15–60 min; ship speed, 6.5–9.3 km h^{-1} (3.5–5.0 kn). We conducted three trawl hauls per day at depths < 40 m. At each station, fish species were identified on board, and the catch was weighed by species. Up to 380 individuals of each species were randomly selected from the trawl catch and stored at –25 °C. Sampled fish were measured to the nearest 0.01 cm fork length for chub mackerel, and standard length for Japanese sardine and Japanese anchovy in the laboratory.

Acoustic data were collected during trawling using a Simrad EK60 scientific echosounder (SIMRAD Kongsberg Maritime AS, Horten, Norway) equipped with a hull-mounted transducer, at an operating frequency of 38 kHz. The echosounder was calibrated in accordance with standard procedures before each survey (Foote, 1987). During operation, the pulse duration and ping interval were set to 1.024 ms and 0.7–1.3 s, respectively.

Conductivity–temperature–depth (CTD) water column profiles were collected at each station. The CTD profiles were used to determine sound speed (Mackenzie, 1981) and absorption coefficient (Francois & Garrison, 1982) for processing of acoustic data.

To analyse schools dominated by one species rather than mixed-species schools, we used only data corresponding to trawl catches where more than 80% of the trawl catch (by weight) was composed of one species (chub mackerel, Japanese sardine, or Japanese anchovy), and where catch exceeded 10 kg. Additionally, because the species of interest tend to disperse in layers at night, making it very difficult to accurately delineate separate schools (Coetzee, 2000), we used only data from daytime trawls.

2.2 Acoustic data processing

The analysis of acoustic data (volume backscattering strength [dB re 1 m^{-1}]) was performed with Echoview (version 11.1; Echoview Software Pty Ltd, Hobart, Australia). To avoid potential surface noise (e.g., wave generated bubbles) and to account for near-field effects, acoustic data shallower than 7.5 m were removed. We also removed data deeper than 50 m because schools of the species of interest rarely extend deeper than 50 m in the study area (the centres of schools of the species were mainly shallower than 30 m [Table 1]). Additionally, manual inspection was used to remove any remaining undesired data (e.g., reverberation, bubble noise). To remove small spikes, two convolution kernels were applied, characterized

by a 3 × 3 median filter and a 5 × 5 dilation filter (Aronica *et al.*, 2019; Fernandes, 2009). A minimum threshold of –60 dB was applied to pre-processed echograms to distinguish fishes from other particulate targets such as plankton (Jech & Michaels, 2006).

For subsequent analyses, we calculated the mean target strength (dB re 1 m^2) of each school and at each station. Target strength indicates the acoustic reflectivity of the ensonified target (e.g., a fish). The mean target strength was calculated from the mean total length of catch samples using the following equations. For chub mackerel (Simmonds & MacLennan, 2008), the equation is:

$$\overline{TS} = 20 \log_{10} \overline{L_t} - 67.6$$

and for Japanese sardine and Japanese anchovy (Zhao *et al.*, 2008), the equation is:

$$\overline{TS} = 20 \log_{10} \overline{L_t} - \frac{20}{3} \log_{10} \left(1 + \frac{\bar{z}}{10}\right) - 70.9$$

where $\overline{L_t}$ is the mean total length (cm) of a catch sample at a given station. For the mean target strength at a station, $\bar{z}$ is defined as the mean depth (m) of the distribution of Japanese sardine or Japanese anchovy at the station, and for the mean target strength in a school, $\bar{z}$ is defined as the mean depth of the school. The mean depth is the average of all sample depths at the station or in the school weighted by volume-backscattering coefficient values. Because body length was measured as fork length (L_f) for chub mackerel, and standard length (L_s) for Japanese sardine and Japanese anchovy, measurements were converted to total length (L_t) by using the following formulae (Furuichi *et al.*, 2021): $L_t = 1.07L_f - 0.136$ for chub mackerel; $L_t = 1.13L_s + 0.371$ for Japanese sardine; and $L_t = 1.12L_s + 0.358$ for Japanese anchovy.

We calculated local population density (ind. m^{-3}) at each station by using the following formula: $D = 10^{(\overline{SV}_{station} - \overline{TS})/10}$, where D is the local population density at a station, $\overline{SV}_{station}$ is the mean volume-backscattering strength of the water column (7.5–50.0 m) during trawling at the station, and $\overline{TS}$ is the mean target strength at the station (Simmonds & MacLennan, 2008).

Fish schools were detected and isolated from the pre-processed echograms by using the Shoals Analysis and Patch Estimation System (SHAPES) algorithm, implemented in Echoview (Barange, 1994; Coetzee, 2000). In the SHAPES algorithm, schools are detected by first identifying candidates, which are groups of adjacent pixels that meet minimum criteria for length and thickness. These individual school candidates are then linked together to form a larger school candidate if the horizontal and vertical distances between them are less than the specified maximum linking distances. After all linking has been carried out, schools are recognized if the final school candidates are larger than the defined minimum total school length and thickness. The detection parameters we used were as follows: minimum total school length, 4 m; minimum school height, 2 m; minimum candidate length, 2 m; minimum candidate height, 1 m; maximum vertical linking distance, 5 m; and maximum horizontal linking distance, 15 m. This set of parameters was selected based on previous studies and the resolution of the acoustic data (Coetzee, 2000; D'Elia *et al.*, 2014; Fernandes, 2009).

All detected schools were classified as chub mackerel, Japanese sardine, or Japanese anchovy based on the trawl catch composition. We extracted school packing density (number of individuals m^{-3}), school volume (m^3), and cross-sectional area (m^2) for each school. The packing density of a school was calculated as $\rho = 10^{(\overline{SV}_{school} - \overline{TS})/10}$, where ρ is the packing density of a school, $\overline{SV}_{school}$ is the mean volume-backscattering strength of the school, and $\overline{TS}$ is the mean target strength in the school (Simmonds & MacLennan, 2008). The volume of a school was calculated assuming a cylindrical shape as $V = \sum_i \pi \cdot (T_i/2)^2 \cdot L_i$, where V is

volume, T_i is the thickness of the school at ping i, and L_i is the distance from ping i to ping $i+1$. School size (number of individuals) was calculated by multiplying the packing density by school volume. In addition, we also calculated the number of schools at each station.

2.3 Statistical analysis

We examined relationships between local population density and school characteristics (school size, number of schools, packing density, school volume, cross-sectional area). To consider the possible nonlinearity of the relationships, we applied power-law models:

$$\mu = a \times x^b$$

where μ is the mean value of a school characteristic (school size, number of schools per km, packing density, school volume, or cross-sectional area), x is local population density, a is a coefficient (>0), and b is a power exponent. The power exponent b determines the direction (positive, constant, or negative) and shape (linear or nonlinear) of the relationship. A negative power exponent ($b < 0$) means a negative relationship between local population density and a school characteristic, an exponent of zero ($b = 0$) means that a school characteristic is constant regardless of local population density, and a positive exponent ($b > 0$) means a positive relationship. Additionally, the power exponent also determines the shape of the relationship when the exponent is greater than zero: an exponent greater than one ($1 < b$) generates a convex relationship (accelerating increase with increasing local population density), an exponent equal to one ($b = 1$) generates a linear relationship (proportionality), and an exponent lower than one ($0 < b < 1$) generates a concave relationship (slowing increase with increasing local population density). The coefficient a

serves as a simple scaling factor, meaning that the shape of the relationship will not change depending on the coefficient, but its placement will move up or down as the coefficient increases or decreases, respectively.

For school size, packing density, school volume, and cross-sectional area, we assumed that observed values follow a Gamma distribution because of their continuous, non-negative, and right-skewed distributions. Therefore, the models were defined as follows:

$$y_{i,j,k} \sim \mathrm{Gamma}\left(\alpha_i, \beta_{i,j}\right)$$

$$\beta_{i,j} = \alpha_i / \mu_{i,j}$$

$$\mu_{i,j} = a_i \times x_{i,j}^{b_i} \times r_l$$

where $y_{i,j}$ is the observed value of a school characteristic of species i at station j in school k, α_i is a shape parameter (>0), $\beta_{i,j}$ is a rate parameter (>0), $\mu_{i,j}$ is the expected (mean) value of the school characteristic, $x_{i,j}$ is local population density, a_i is a coefficient, b_i is a power exponent, and r_l is a random effect of date l. Factors other than population density have also been reported to affect schooling behaviour (Borner *et al.*, 2015; Romenskyy *et al.*, 2020; Zheng & Fu, 2021), and these factors may cause spatiotemporal autocorrelation in school characteristics. To consider this spatiotemporal autocorrelation, survey date was incorporated into the model as a multiplicative random effect following a normal distribution with mean 1 and standard deviation σ_r^2. To avoid overfitting and obtain a more reliable and robust estimate, we assumed that the parameters a_i, b_i, and α_i have hierarchical prior distributions (that is, a hierarchical modelling framework was applied). The prior distributions of a_i, b_i, and α_i were defined as normal distributions with means a_0, b_0, and α_0 and standard deviations σ_a^2, σ_b^2, and σ_α^2, respectively.

For the number of schools, we assumed that observed values followed a negative binomial distribution because the data were count data characterized by a large variance. Therefore, the model was defined as follows:

$$y_{i,j} \sim \mathrm{NegativeBinomial}\left(\lambda_{i,j}, \varphi_i\right)$$

$$\lambda_{i,j} = d_{i,j} \times \mu_{i,j}$$

$$\mu_{i,j} = a_i \times x_{i,j}^{b_i} \times r_l$$

where $y_{i,j}$ is the observed number of schools of species i at station j, $\lambda_{i,j}$ is a location parameter (>0), φ_i is a dispersion parameter (>0), $d_{i,j}$ is sampling distance (km), $\mu_{i,j}$ is the expected (mean) number of schools per km, $x_{i,j}$ is local population density, a_i is a coefficient, b_i is a power exponent, and r_l is a random effect of date l. To consider any spatiotemporal autocorrelation, survey date was incorporated into the model as a multiplicative random effect following a normal distribution with mean 1 and standard deviation σ_r^2. To avoid overfitting and obtain a more reliable and robust estimate, we assumed that the parameters a_i, b_i, and φ_i have hierarchical prior distributions. The prior distributions of a_i, b_i, and φ_i were defined as normal distributions with means a_0, b_0, and φ_0 and standard deviations σ_a^2, σ_b^2, and σ_φ^2, respectively.

Furthermore, we investigated whether the relationships between local population density and school characteristics are different or common among species. In addition to the above models assuming species-specific relationships, we also constructed models assuming species-common relationships, where the coefficient and power exponent were same among species, that is, $a_{mackerel} = a_{sardine} = a_{anchovy}$ and $b_{mackerel} = b_{sardine} = b_{anchovy}$. To compare models, the widely applicable Bayesian information criterion (WBIC) was

calculated for each model (Watanabe, 2013).

We fitted the models in a Bayesian framework using Markov chain Monte Carlo methods via No-U-Turn sampling with the software STAN, which was called from R (R Development Core Team, 2020) using the package 'rstan' (Stan Development Team, 2020), to obtain posterior parameter distributions. We used weak informative priors (Cauchy or half-Cauchy distribution with location parameter 0 and scale parameter 5) for all parameters except σ_r^2. For σ_r^2, a normal distribution with mean 0 and standard deviation 0.2 was used as the prior distribution because of the difficulty in converging. We used four chains, each of which had 20,000 iterations including a burn-in of 10,000 iterations with a thinning interval of two, resulting in 20,000 values for the posterior distribution of each parameter. Convergence of Markov chain Monte Carlo algorithms was checked by using the potential scale reduction statistic ($\hat{R}$) and effective sample sizes (Carpenter *et al.*, 2017); for all parameters, the $\hat{R}$ was less than 1.01 and effective sample sizes were greater than 400.

2.4 Ethical statement

All samples in this study were obtained from fisheries surveys, and animal experiments that require permits pertinent to animal welfare regulations were not conducted. Chub mackerel, Japanese sardine, and Japanese anchovy in the study area are not endangered and are managed through the stock assessment process in Japan.

3. RESULTS

In total, data from 88 stations and 518 schools were obtained (Table 1). A wide range of local population density (ind. m^{-3}) was observed ranging from 4.6×10^{-6} to 0.016 for chub mackerel, from 1.26×10^{-4} to 0.58 for Japanese sardine, and from 1.18×10^{-4} to 0.41 for

Japanese anchovy.

3.1 School size

For all species, school size tended to increase as local population density increased, and the power exponents were greater than zero, indicating positive relationships (Figures 2a and 3, and Table S1). In each case, the estimated power exponents were close to but less than one, and the credible intervals did not include one (Figure 2a and Table S1). This indicates that school size increased almost linearly with local population density, but the rate of increase slowed slightly as local population size increased. The model with species-specific relationships between school size and population density had a lower WBIC than the model with species-common relationships (species-specific, 40.2; species-common, 48.9), indicating that the relationships differed among species.

3.2 Number of schools

For all species, the number of schools per km tended to increase as local population density increased, but the rate of increase slowed with increasing local population density (Figure 4). For all species, the power exponents were greater than zero (indicating positive relationships) but much less than one (ranging from 0.33 to 0.39; Figure 2b and Table S1), indicating that the rate of increase of the number of schools slowed considerably with increasing local population density (Figure 4). The model with species-specific relationships between the number of schools and population density had a lower WBIC than the model with species-common relationships (species-specific, 224.0; species-common, 225.8), indicating that the relationships differed among species.

3.3 School packing density

In all species, packing density tended to increase as local population density increased, but the rate of increase slowed with increasing population density (Figure 5). For all species, the power exponents were greater than zero (indicating positive relationships) but much less than one (ranging from 0.32 to 0.40; Figure 2c and Table S1), indicating that the rate of increase of packing density slowed considerably with increasing local population (Figure 5). The model with species-specific relationships between packing density and population density had a lower WBIC than the model with species-common relationships (species-specific, 455.9; species-common, 460.2), indicating that the relationships differed among species.

3.4 Spatial extent of a school

For all species, school volume tended to increase with increasing local population density, but the rate of increase slowed as population density increased (Figure 6). For all species, the power exponents were greater than zero (indicating positive relationships) but much less than one (ranging from 0.25 to 0.37; Figure 2d and Table S1), indicating that the rate of increase of school volume slowed considerably with increasing local population (Figure 6). The model with species-specific relationships between school volume and population density had a lower WBIC than the model with species-common relationships (species-specific, 207.8; species-common, 210.4), indicating that the relationships differed among species.

In school cross-sectional area, for all species, the power exponents were greater than zero (indicating positive relationships) but much less than one (ranging from 0.16 to 0.24; Figure 2e and Table S1), indicating that the rate of increase of cross-sectional area slowed considerably with increasing local population (Figure 7). The model with species-specific relationships between cross-sectional area and population density had a lower WBIC than the model with species-common relationships (species-specific, 690.6; species-common, 693.1), indicating that the relationships differed among species.

4. DISCUSSION

The effects of population density on school size and the number of schools is important for understanding population dynamics, community structure, and energy flow in marine ecosystems because the school is a fundamental ecological unit in which biological interactions such as competition and predation take place (Maury, 2017; Maury & Poggiale, 2013). However, information on the relationships between population density and school characteristics among small pelagic fishes in the field remains scarce, and quantitative relationships are yet to be clarified. In the present study, we show that school size increases almost linearly with population density, whereas the number of schools increases non-linearly in such a way that the rate of increase slows considerably with increasing population density. Our study provides important information on the quantitative relationships between population density and school characteristics.

Our results are largely consistent with the predictions of a theoretical model based on simple assumptions of encounter, merge, and split processes (Niwa, 2004). In the model, schools are assumed to move at random through their environment. Schools merge whenever they encounter another school, and each school splits periodically into two schools. The schooling process of the studied species may resemble this simple model. However, there is a slight difference between our results and the predictions of the model. Whereas the model predicts that mean school size will increase linearly with population density, our results show that the rate of increase of mean school size slowed slightly with increasing local population size (i.e., a near-linear relationship), implying the existence of an optimal (stable) school size. The reason for this difference is likely that the theoretical model is purely mechanistic and does not consider the functions (i.e., the ultimate factors) of schooling behaviour. The

formation of schools involves not only benefits but also costs, leading to the existence of an optimal group size that allows individuals to maximize their net benefit (Krause & Ruxton, 2002; Ward & Webster, 2016), and it has been suggested that individuals adjust their schooling behaviour to increase their net benefit (Sibly, 1983). Accordingly, in our study species, the probability of school merging and splitting likely changed with school size in a way that served to increase this net benefit (Gueron & Levin, 1995; Niwa, 1998). A combination of mechanistic and functional approaches will be needed in future studies to better understand the dynamics of school size (Griesser *et al.*, 2011; Sumpter, 2010).

Our results show that whereas at low population densities, increasing density resulted in both more and larger schools, at high population densities, increasing density resulted in larger schools rather than more schools. This can be explained by the following mechanism: at low population densities, the frequency of encounters with conspecific schools is low, and hence many small schools are formed, whereas at high population densities, the frequency of encounter with conspecific schools is high, and as many schools merge to form larger schools, the number of schools becomes relatively stable. Similar trends have also been found in freshwater cyprinid fishes and terrestrial mammals, which form much smaller groups than marine small pelagic fishes (Holubová *et al.*, 2019; Pépin & Gerard, 2008; Southwell, 1984). This suggests that this pattern might be widespread in animals that form fluid groups.

Our results also show that school packing density increased with increasing population density. This suggests that school size and packing density increase simultaneously as population densities increase. In fact, school size and packing density were strongly correlated (chub mackerel: $\rho = 0.75$, $p < 0.001$; Japanese sardine: $\rho = 0.82$, $p < 0.001$; Japanese anchovy: $\rho = 0.79$, $p < 0.001$). For small to mid-sized schools, predation risk per individual is expected to decrease as school size increases (Caro, 2005; Krause & Ruxton, 2002; Lima, 1995). For large schools, however, as school size increases, the risk of predator attacks also increases as

the school becomes more visible to predators (Maury, 2017; Pitcher & Parrish, 1993). Denser schools can engage in highly coordinated antipredator reactions through the efficient transmission of information within schools (Rieucau *et al.*, 2014a, 2014b), and therefore, the formation of dense schools could be a response of individuals against the threat of predation. Small pelagic fishes form especially massive schools, and individuals might cope with the increased risk of predator attacks at these large school sizes by forming dense and compact schools that allow them to efficiently obtain information from other schooling individuals.

In small pelagic fishes, a strong density-dependent decline in body growth is often observed during times of increasing population density (Canales *et al.*, 2020; Kamimura *et al.*, 2021a; Wada *et al.*, 1995; Watanabe & Yatsu, 2004). Density-dependent growth reduction is mainly caused by intraspecific competition for food (Hansen *et al.*, 1999; Jenkins *et al.*, 1999; Kamimura *et al.*, 2021a; Post *et al.*, 1999). Food competition can occur between schools and within a school, but within-school competition is likely to be stronger and more direct than between-school competition. Several studies in animals that form groups (although none of the studies were conducted on fish) have reported that competition for food within groups is more intense than competition between groups (Janson, 1985, 1988). The increase in school size and packing density with increasing population density observed in our study is likely to create fairly strong competition for food. This might be one of the reasons for the strong negative density-dependence of growth observed in small pelagic fishes.

In our study, the shapes of the relationships between population density and school characteristics differed among small pelagic fishes (although the overall trends were similar across species). In krill, which are similar to small pelagic fishes in that they often form massive swarms and are preyed upon by a wide variety of pelagic megafauna, it has been reported that increasing population density causes a linear increase in the number of schools, but does not affect school size (Brierley & Cox, 2015). This is different from the relationships

observed in small pelagic fishes in our study. Differences in selection pressures (e.g., competition and predation) can lead to differences in optimal school size and hence to differences in aggregation tendency (i.e., the frequency of school fission and fusion) (Rieucau *et al.*, 2015). This may account for the different shapes of the relationships between population density and school characteristics among species and taxa.

Furthermore, relationships between population density and school characteristics could also vary within a species depending on several factors. For example, seasonality (e.g., spawning and feeding seasons), body size, and age can affect optimal school sizes and aggregation tendencies (Croft *et al.*, 2003; Hoare *et al.*, 2000; Makris *et al.*, 2009). Our study was conducted during the feeding season, and variations of body size and age in the study area were small throughout the study period (2007–2021). The body lengths of most chub mackerel and Japanese sardine corresponded to those of young of the year (Kamimura *et al.*, 2021a, 2021b). Further studies across seasons, locations, body sizes, ages, and species are needed to identify general patterns in relationships between population density and school characteristics.

Our results will be useful for population-status assessment of these species. Population density was positively correlated with school characteristics, indicating that school characteristics could be used as an indicator of population status. However, the relationships were highly nonlinear (except for that of school size). Therefore, this nonlinearity should be taken into account when using school characteristics as an indicator of population status (Erisman *et al.*, 2011).

In the present study, we inferred schooling characteristics from echosounder data. Echosounder signals provide information in two dimensions: vertically through the water column and horizontally with successive acoustic signals along the vessel track (Simmonds & MacLennan, 2008). This means that we were able to sample only a small fraction of each

school we identified. In fact, several schools were estimated to be quite small. A previous study has reported that there are no significant differences between schooling characteristics obtained from echosounders and multibeam sonar, which can image an entire school in three dimensions (Brierley & Cox, 2015). Therefore, the overall trend in our results is likely to be robust. However, the use of methods that can obtain three-dimensional data (e.g., multibeam sonar) will enable more accurate and detailed analysis (Paramo *et al.*, 2007) in the future and could provide new biological and ecological insights.

In conclusion, our results show that school size increased almost linearly with increasing population density, whereas the number of schools and other school characteristics (school packing density, school volume, and school cross-sectional area) increased non-linearly such that the rate of increase slowed considerably with increasing population density. Furthermore, we found that the shapes of the relationships between population density and school characteristics differed among species, although the overall trend was similar. These results indicate that the schooling behaviour of small pelagic fish species is density-dependent, and responses to changes in density differ among species. Our results will help advance understanding of how biological interactions such as intra- and inter-specific competition and predator–prey interactions mediate the density-dependent processes that underlie the population dynamics and community structure of small pelagic fishes in marine ecosystems (Maury, 2017).

ACKNOWLEDGEMENTS

The dataset analysed in this study was made possible by enormous efforts undertaken by numerous researchers, as well as the captains, officers, and crews of the training vessel *Hokuho-Maru*. We also thank English-speaking professional editors from ELSS, Inc., for English proofreading.

AUTHOR CONTRIBUTIONS

S.F. conceived of the study and performed data analysis. S.F., Y.K., M.S., and R.Y. contributed to data collection. S.F. wrote the manuscript with support from Y.K., M.S., and R.Y.. All authors discussed the results and contributed to the final manuscript. R.Y. supervised the survey.

REFERENCES

Aronica, S., Fontana, I., Giacalone, G., Lo Bosco, G., Rizzo, R., Mazzola, S., Basilone, G., Ferreri, R., Genovese, S., Barra, M., & Bonanno, A. (2019). Identifying small pelagic Mediterranean fish schools from acoustic and environmental data using optimized artificial neural networks. *Ecological Informatics*, **50**, 149–161.

Bakun, A. (2006). Wasp-waist populations and marine ecosystem dynamics: Navigating the 'predator pit' topographies. *Progress in Oceanography*, **68**, 271–288.

Barange, M. (1994). Acoustic identification, classification and structure of biological patchiness on the edge of the Agulhas Bank and its relation to frontal features. *South African Journal of Marine Science*, **14**, 333–347.

Borner, K. K., Krause, S., Mehner, T., Uusi-Heikkilä, S., Ramnarine, I. W., & Krause, J. (2015). Turbidity affects social dynamics in Trinidadian guppies. *Behavioral Ecology and Sociobiology*, **69**, 645–651.

Brierley, A. S., & Cox, M. J. (2015). Fewer but not smaller schools in declining fish and krill populations. *Current Biology*, **25**, 75–79.

Canales, T. M., Delius, G. W., & Law, R. (2020). Regulation of fish stocks without stock–recruitment relationships: the case of small pelagic fish. *Fish and Fisheries*, **21**, 857–871.

Caro, T. (2005). *Antipredator defenses in birds and mammals*. Chicago, IL: University of Chicago Press.

Carpenter, B., Gelman, A., Hoffman, M. D., Lee, D., Goodrich, B., Betancourt, M., Brubaker, M. A., Guo, J., Li, P., & Riddell, A. (2017). Stan: A probabilistic programming language. *Journal of Statistical Software*, **76**.

Coetzee, J. (2000). Use of a shoal analysis and patch estimation system (SHAPES) to

characterise sardine schools. *Aquatic Living Resources*, **13**, 1–10.

Croft, D. P., Krause, J., Couzin, I. D., & Pitcher, T. J. (2003). When fish shoals meet: outcomes for evolution and fisheries. *Fish and Fisheries*, **4**, 138–146.

Cury, P., Bakun, A., Crawford, R. J. M., Jarre, A., Quiñones, R. A., Shannon, L. J., & Verheye, H. M. (2000). Small pelagics in upwelling systems: Patterns of interaction and structural changes in 'wasp-waist' ecosystems. *ICES Journal of Marine Science*, **57**, 603–618.

D'Elia, M., Patti, B., Bonanno, A., Fontana, I., Giacalone, G., Basilone, G., & Fernandes, P. G. (2014). Analysis of backscatter properties and application of classification procedures for the identification of small pelagic fish species in the Central Mediterranean. *Fisheries Research*, **149**, 33–42.

Erisman, B. E., Allen, L. G., Claisse, J. T., Pondella, D. J., Miller, E. F., & Murray, J. H. (2011). The illusion of plenty: Hyperstability masks collapses in two recreational fisheries that target fish spawning aggregations. *Canadian Journal of Fisheries and Aquatic Sciences*, **68**, 1705–1716.

Fernandes, P. G. (2009). Classification trees for species identification of fish-school echotraces. *ICES Journal of Marine Science*, **66**, 1073–1080.

Foote, K. G. (1987). Fish target strengths for use in echo integrator surveys. *Journal of the Acoustical Society of America*, **82**, 981–987.

Francois, R. E., & Garrison, G. R. (1982). Sound absorption based on ocean measurements. Part II: Boric acid contribution and equation for total absorption. *Journal of the Acoustical Society of America*, **72**, 1879–1890.

Furuichi, S., Kamimura, Y., & Yukami, R. (2021). Length–length and length–weight relationships for four dominant small pelagic fishes in the Kuroshio–Oyashio current system. *Thalassas: An International Journal of Marine Sciences*, **37**, 651–657.

Griesser, M., Ma, Q., Webber, S., Bowgen, K., & Sumpter, D. J. T. (2011). Understanding animal group-size distributions. *PLoS ONE*, **6**, e23438.

Gueron, S., & Levin, S. A. (1995). The dynamics of group formation. *Mathematical Biosciences*, **128**, 243–264.

Hansen, T. F., Stenseth, N. C., Henttonen, H., & Tast, J. (1999). Interspecific and intraspecific competition as causes of direct and delayed density dependence in a fluctuating vole population. *Proceedings of the National Academy of Sciences of the United States of America*, **96**, 986–991.

Hensor, E., Couzin, I. D., James, R., & Krause, J. (2005). Modelling density-dependent fish shoal distributions in the laboratory and field. *Oikos*, **110**, 344–352.

Hoare, D. J., Krause, J., Peuhkuri, N., & Godin, J.-G. J. (2000). Body size and shoaling in fish. *Journal of Fish Biology*, **57**, 1351–1366.

Holubová, M., Čech, M., Vašek, M., & Peterka, J. (2019). Density dependent attributes of fish aggregative behaviour. *PeerJ*, **2019**, e6378.

Janson, C. (1985). Aggresive competition and individual food consumption in wild brown capuchin monkeys (*Cebus apella*). *Behavioral Ecology and Sociobiology*, **18**, 125–138.

Janson, C. H. (1988). Food competition in brown capuchin monkeys (*Cebus apella*): quantitative effects of group size and tree productivity. *Behaviour*, **105**, 53–76.

Jech, J. M., & Michaels, W. L. (2006). A multifrequency method to classify and evaluate fisheries acoustics data. *Canadian Journal of Fisheries and Aquatic Sciences*, **63**, 2225–2235.

Jech, J. M., & Stroman, F. (2012). Aggregative patterns of pre-spawning Atlantic herring on Georges Bank from 1999-2010. *Aquatic Living Resources*, **25**, 1–14.

Jenkins, T. M., Diehl, S., Kratz, K. W., & Cooper, S. D. (1999). Effects of population density

on individual growth of brown trout in streams. *Ecology*, **80**, 941–956.

Kamimura, Y., Taga, M., Yukami, R., Watanabe, C., & Furuichi, S. (2021a). Intra- and inter-specific density dependence of body condition, growth, and habitat temperature in chub mackerel (Scomber japonicus). *ICES Journal of Marine Science*, **78**, 3254–3264.

Kamimura, Y., Tadokoro, K., Furuichi, S., & Yukami, R. (2021b). Stronger density-dependent growth of Japanese sardine with lower food availability: Comparison of growth and zooplankton biomass between a historical and current stock-increase period in the western North Pacific. *bioRxiv*, 2021.12.26.474216.

Krause, J., & Ruxton, G. D. (2002). *Living in groups*. Oxford: Oxford University Press.

Lima, S. L. (1995). Back to the basics of anti-predatory vigilance: the group-size effect. *Animal Behaviour*, **49**, 11–20.

Mackenzie, K. V. (1981). Nine-term equation for sound speed in the oceans. *Journal of the Acoustical Society of America*, **70**, 807–812.

Makris, N. C., Ratilal, P., Jagannathan, S., Gong, Z., Andrews, M., Bertsatos, I., Godo, O. R., Nero, R. W., & Jech, J. M. (2009). Critical population density triggers rapid formation of vast oceanic fish shoals. *Science*, **323**, 1734–1737.

Makris, N. C., Ratilal, P., Symonds, D. T., Jagannathan, S., Lee, S., & Nero, R. W. (2006). Fish population and behavior revealed by instantaneous continental shelf-scale imaging. *Science*, **311**, 660–663.

Maury, O. (2017). Can schooling regulate marine populations and ecosystems? *Progress in Oceanography*, **156**, 91–103.

Maury, O., & Poggiale, J. C. (2013). From individuals to populations to communities: A dynamic energy budget model of marine ecosystem size-spectrum including life history diversity. *Journal of Theoretical Biology*, **324**, 52–71.

Misund, O. (1993). Dynamics of moving masses: variability in packing density, shape, and size among herring, sprat, and saithe schools. *ICES Journal of Marine Science*, **50**, 145–160.

Niwa, H.-S. (2004). Space-irrelevant scaling law for fish school sizes. *Journal of Theoretical Biology*, **228**, 347–357.

Niwa, H. S. (1998). School size statistics of fish. *Journal of Theoretical Biology*, **195**, 351–361.

Paramo, J., Bertrand, S., Villalobos, H., & Gerlotto, F. (2007). A three-dimensional approach to school typology using vertical scanning multibeam sonar. *Fisheries Research*, **84**, 171–179.

Pavlov, D. S., & Kasumyan, A. O. (2000). Patterns and mechanisms of schooling behavior in fish: a review. *Journal of Ichthyology*, **40**, S163.

Pépin, D., & Gerard, J. F. (2008). Group dynamics and local population density dependence of group size in the Pyrenean chamois, *Rupicapra pyrenaica*. *Animal Behaviour*, **75**, 361–369.

Petitgas, P., Reid, D., Carrera, P., Iglesias, M., Georgakarakos, S., Liorzou, B., & Massé, J. (2001). On the relation between schools, clusters of schools, and abundance in pelagic fish stocks. *ICES Journal of Marine Science*, **58**, 1150–1160.

Pitcher, T. J., & Parrish, J. K. (1993). Functions of shoaling behaviour in teleosts. In T. J. Pitcher (Ed.), *The behaviour of teleost fishes* (pp. 263–439). Chapman and Hall.

Post, J. R., Parkinson, E. A., & Johnston, N. T. (1999). Density-dependent processes in structured fish populations: interaction strengths in whole-lake experiments. *Ecological Monographs*, **69**, 155–175.

R Development Core Team. (2020). *R: A language and environment for statistical computing*.

R Foundation for Statistical Computing, Vienna, Austria.

Rice, J. (1995). Food web theory, marine food webs, and what climate change may do to northern fish populations. *Canadian Special Publication of Fisheries and Aquatic Sciences*, **121**, 561–568.

Rieucau, G., Boswell, K. M., De Robertis, A., Macaulay, G. J., & Handegard, N. O. (2014a). Experimental evidence of threat-sensitive collective avoidance responses in a large wild-caught herring school. *PLoS ONE*, **9**, e86726.

Rieucau, G., De Robertis, A., Boswell, K. M., & Handegard, N. O. (2014b). School density affects the strength of collective avoidance responses in wild-caught Atlantic herring *Clupea harengus*: a simulated predator encounter experiment. *Journal of Fish Biology*, **85**, 1650–1664.

Rieucau, G., Fernö, A., Ioannou, C. C., & Handegard, N. O. (2015). Towards of a firmer explanation of large shoal formation, maintenance and collective reactions in marine fish. *Reviews in Fish Biology and Fisheries*, **25**, 21–37.

Romenskyy, M., Herbert-Read, J. E., Ioannou, C. C., Szorkovszky, A., Ward, A. J. W., & Sumpter, D. J. T. (2020). Quantifying the structure and dynamics of fish shoals under predation threat in three dimensions. *Behavioral Ecology*, **31**, 311–321.

Sibly, R. M. (1983). Optimal group size is unstable. *Animal Behaviour*, **31**, 947–948.

Simmonds, J., & MacLennan, D. N. (2008). *Fisheries acoustics: theory and practice*, second edi. Oxford, UK: Blackwell Publishing.

Southwell, C. J. (1984). Variability in grouping in the eastern grey kangaroo, *Macropus giganteus* I. Group density and group size. *Wildlife Research*, **11**, 423–435.

Stan Development Team. (2020). *Stan: the R interface to Stan. R package version 2.19.2*.

Sumpter, D. J. T. (2010). *Collective animal behavior*. Princeton University Press.

Vicsek, T., & Zafeiris, A. (2012). Collective motion. *Physics Reports*, **517**, 71–140.

Wada, T., Matsubara, T., Matsumiya, Y., & Koizumi, N. (1995). Influence of environment of stock fluctuations of Japanese sardine, Sardinops melanostictus. *Canadian Special Publication of Fisheries and Aquatic Sciences*, **121**, 387–394.

Ward, A., & Webster, M. (2016). *Sociality: The behaviour of group-living animals*. Springer International Publishing.

Watanabe, C., & Yatsu, A. (2004). Effects of density-dependence and sea surface temperature on interannual variation in length-at-age of chub mackerel (Scomber japonicus) in the Kuroshio-Oyashio area during 1970-1997. *Fishery Bulletin*, **102**, 206.

Watanabe, S. (2013). A widely applicable bayesian information criterion. *Journal of Machine Learning Research*, **14**, 867–897.

Yatsu, A. (2019). Review of population dynamics and management of small pelagic fishes around the Japanese Archipelago. *Fisheries Science*, **85**, 611–639.

Zhao, X., Wang, Y., & Dai, F. (2008). Depth-dependent target strength of anchovy (*Engraulis japonicus*) measured in situ. *ICES Journal of Marine Science*, **65**, 882–888.

Zheng, Y. H., & Fu, S. J. (2021). Effects of fasting on collective movement and fission–fusion dynamics in both homogeneous and heterogeneous shoals of a group-living cyprinid fish species. *Journal of Fish Biology*, **99**, 1640–1649.

Table 1. Characteristics of detected schools of chub mackerel *Scomber japonicus*, Japanese sardine *Sardinops melanostictus*, and Japanese anchovy *Engraulis japonicus* by year. L_t, total length; Q1, first quartile; Q3, third quartile.

Species	Year	Total number of stations	Total number of schools	School depth (m)		Mean L_t (by station; cm)	
				Median	Q1−Q3	Median	Q1−Q3
Chub mackerel	2010	1	3	14.7	14.4–26.0	21.7	–
Chub mackerel	2013	4	25	19.2	15.0–20.7	19.6	19.2–19.9
Chub mackerel	2014	1	1	22.3	–	23.1	–
Chub mackerel	2015	1	1	19.8	–	19.4	–
Chub mackerel	2016	1	4	21.4	18.0–23.0	18.7	–
Chub mackerel	2018	2	2	18.4	14.9–21.9	24.8	20.6–29.0
Chub mackerel	2019	1	1	18.4	–	25.8	–
Chub mackerel	2020	3	14	25.6	21.9–32.1	19.2	18.6–19.7
Japanese sardine	2014	1	3	25.2	24.6–25.9	15.3	–
Japanese sardine	2015	6	38	18.9	16.6–22.4	15.3	15.3–15.6
Japanese sardine	2017	1	29	20.8	14.9–22.5	14.4	–
Japanese sardine	2018	4	61	16.4	15.7–17.6	13.6	13.4–13.7
Japanese sardine	2019	2	3	20.7	19.5–23.9	14.5	14.2–14.8
Japanese sardine	2020	1	1	19.4	–	14.5	–
Japanese sardine	2021	10	38	23.9	19.8–29.2	14.0	13.6–14.5
Japanese anchovy	2007	1	5	24.6	24.1–27.5	12.7	–
Japanese anchovy	2008	3	21	22.0	18.0–24.7	11.8	11.1–12.2
Japanese anchovy	2009	12	53	26.0	22.4–30.9	12.1	11.6–12.4
Japanese anchovy	2010	10	68	20.0	17.8–23.9	12.8	12.5–13.2
Japanese anchovy	2011	13	92	21.4	19.2–25.4	10.8	10.4–11.8
Japanese anchovy	2012	8	34	19.3	16.7–22.0	13.3	12.9–13.7
Japanese anchovy	2013	2	21	26.1	22.6–27.6	13.0	12.9–13.1

Figure captions

Figure 1. Sampling stations (translucent circles) used for trawl-acoustic surveys in the Pacific Ocean off Japan and the Kuril Islands from 2007 to 2021.

Figure 2. Estimated power exponents for the relationship between local population density and (a) school size, (b) the number of schools, (c) school packing density, (d) school volume, and (e) school cross-sectional area. Points indicate estimated values (posterior means), and error bars indicate 90% credible intervals.

Figure 3. Relationship between local population density and school size for (a) chub mackerel *Scomber japonicus*, (b) Japanese sardine *Sardinops melanostictus*, and (c) Japanese anchovy *Engraulis japonicus*. Translucent circles indicate observed values of individual schools. Solid lines indicate estimated relationships (posterior means), and grey bands indicate 90% credible intervals.

Figure 4. Relationship between local population density and the number of schools for (a) chub mackerel *Scomber japonicus*, (b) Japanese sardine *Sardinops melanostictus*, and (c) Japanese anchovy *Engraulis japonicus*. Translucent circles indicate observed values at individual stations. Solid lines indicate estimated relationships (posterior means), and grey bands indicate 90% credible intervals.

Figure 5. Relationship between local population density and school packing density for (a) chub mackerel *Scomber japonicus*, (b) Japanese sardine *Sardinops melanostictus*, and (c) Japanese anchovy *Engraulis japonicus*. Translucent circles indicate observed values of

individual schools. Solid lines indicate estimated relationships (posterior means), and grey bands indicate 90% credible intervals.

Figure 6. Relationship between local population density and school volume for (a) chub mackerel *Scomber japonicus*, (b) Japanese sardine *Sardinops melanostictus*, and (c) Japanese anchovy *Engraulis japonicus*. Translucent circles indicate observed values of individual schools. Solid lines indicate estimated relationships (posterior means), and grey bands indicate 90% credible intervals.

Figure 7. Relationship between local population density and school cross-sectional area for (a) chub mackerel *Scomber japonicus*, (b) Japanese sardine *Sardinops melanostictus*, and (c) Japanese anchovy *Engraulis japonicus*. Translucent circles indicate observed values of individual schools. Solid lines indicate estimated relationships (posterior means), and grey bands indicate 90% credible intervals.

Figure 1

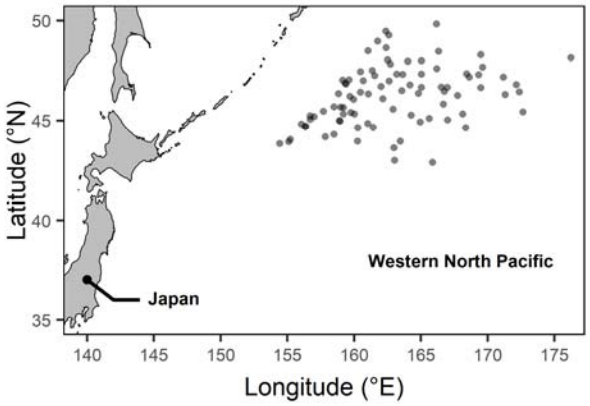
Latitude (°N)
50
45
40
35
Western North Pacific
Japan
140
145
150
155
160
165
170
175
Longitude (°E)

Figure 2

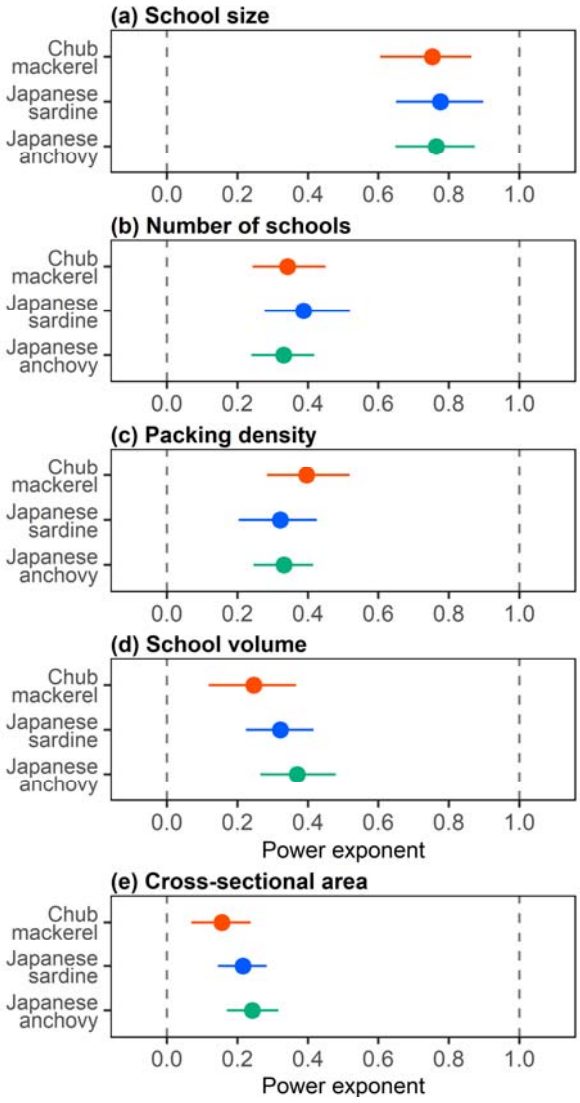
(a) School size
Chub mackerel
Japanese sardine
Japanese anchovy
0.0 0.2 0.4 0.6 0.8 1.0
(b) Number of schools
Chub mackerel
Japanese sardine
Japanese anchovy
0.0 0.2 0.4 0.6 0.8 1.0
(c) Packing density
Chub mackerel
Japanese sardine
Japanese anchovy
0.0 0.2 0.4 0.6 0.8 1.0
(d) School volume
Chub mackerel
Japanese sardine
Japanese anchovy
0.0 0.2 0.4 0.6 0.8 1.0
Power exponent
(e) Cross-sectional area
Chub mackerel
Japanese sardine
Japanese anchovy
0.0 0.2 0.4 0.6 0.8 1.0
Power exponent

Figure 3

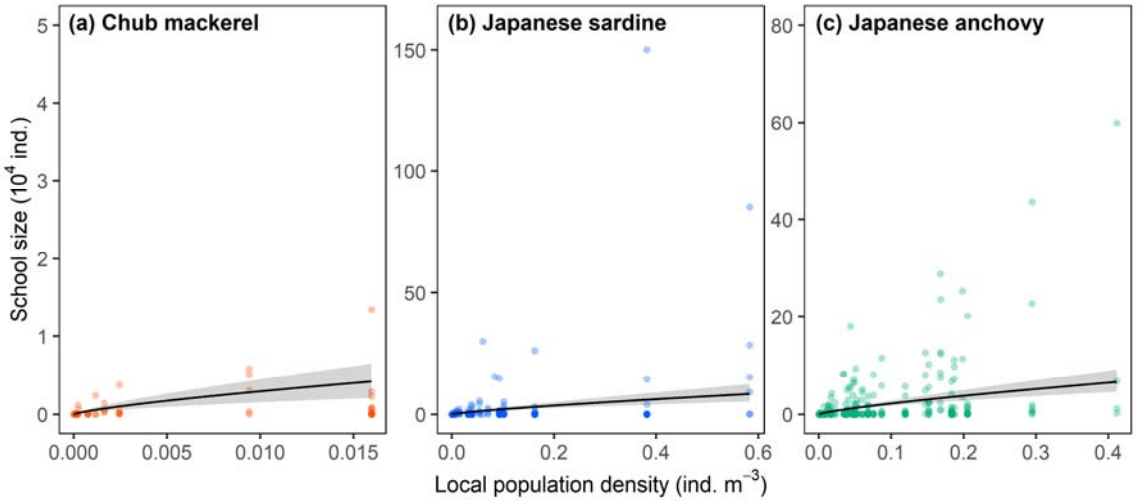
(a) Chub mackerel
(b) Japanese sardine
(c) Japanese anchovy
School size (10^4 ind.)
Local population density (ind. m^{-3})
0
1
2
3
4
5
0.000
0.005
0.010
0.015
0
50
100
150
0.0
0.2
0.4
0.6
0
20
40
60
80
0.0
0.1
0.2
0.3
0.4

Figure 4

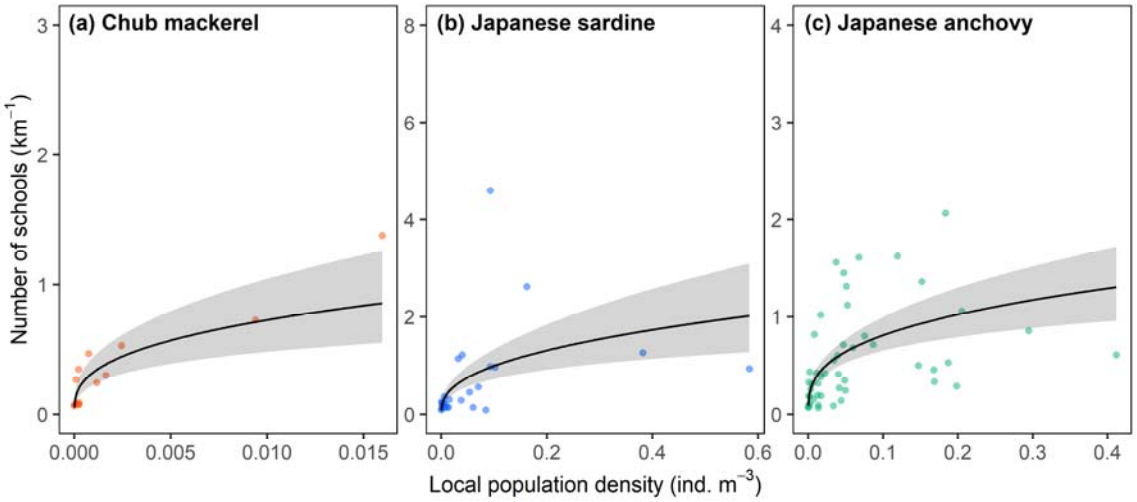
(a) Chub mackerel
(b) Japanese sardine
(c) Japanese anchovy
Number of schools (km^{-1})
Local population density (ind. m^{-3})
0.000
0.005
0.010
0.015
0.0
0.2
0.4
0.6
0.1
0.3

Figure 5

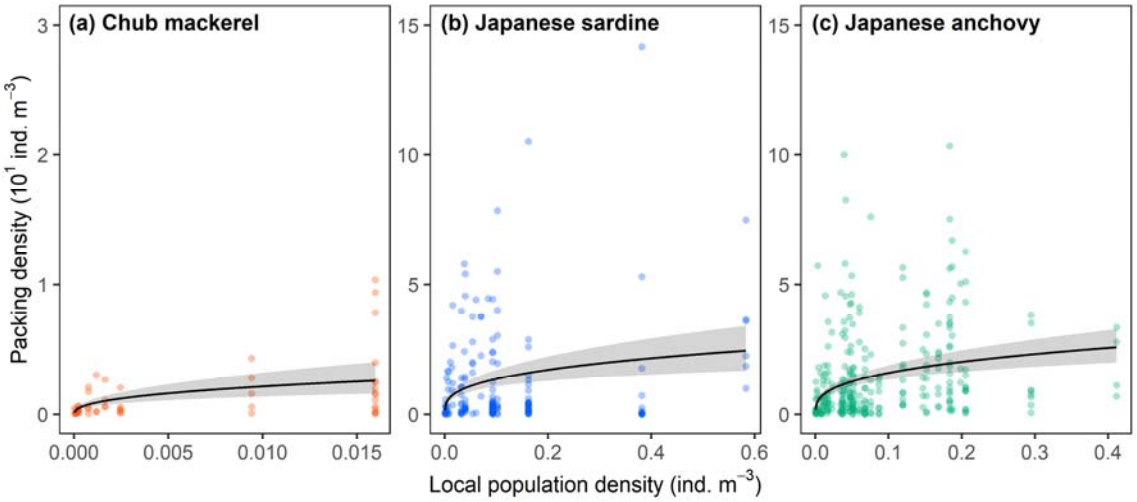
(a) Chub mackerel
(b) Japanese sardine
(c) Japanese anchovy
Packing density (10^1 ind. m^{-3})
Local population density (ind. m^{-3})
0.000
0.005
0.010
0.015
0.0
0.2
0.4
0.6
0.1
0.3
0
1
2
3
5
10
15

Figure 6

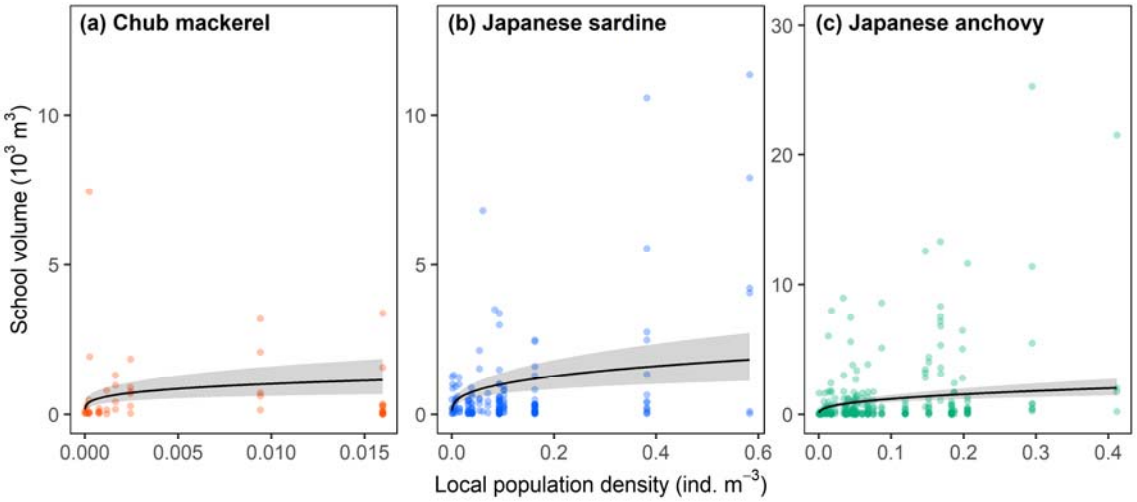
(a) Chub mackerel
(b) Japanese sardine
(c) Japanese anchovy
School volume (10^3 m^3)
Local population density (ind. m^{-3})
0
5
10
20
30
0.000
0.005
0.010
0.015
0.0
0.2
0.4
0.6
0.1
0.3

Figure 7

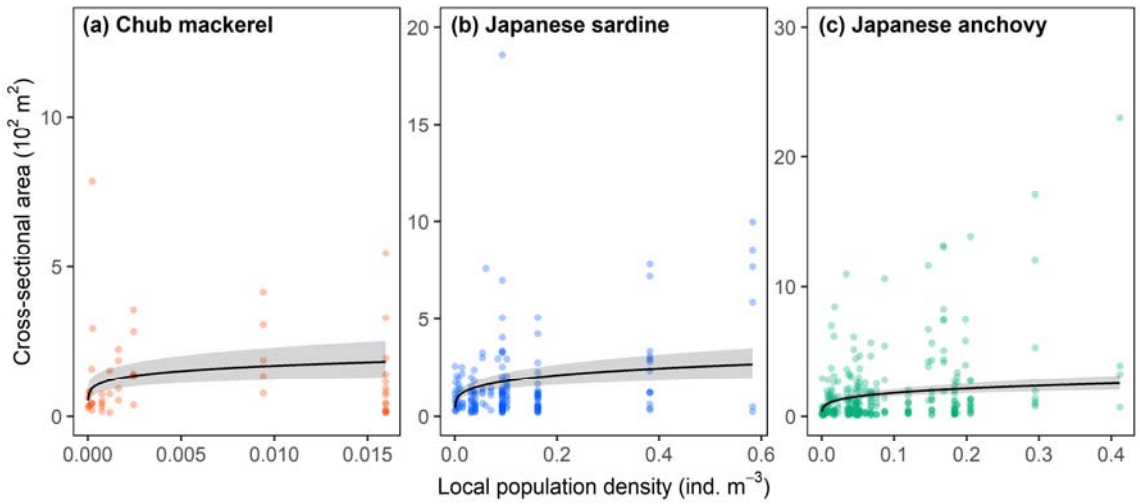
(a) Chub mackerel
(b) Japanese sardine
(c) Japanese anchovy
Cross-sectional area (10^2 m^2)
Local population density (ind. m^{-3})
0
5
10
15
20
30
0.000
0.005
0.010
0.015
0.0
0.2
0.4
0.6
0.1
0.3